J Biomol NMR (2015) 63:229–235
DOI 10.1007/s10858-015-9979-7

NMR STRUCTURE NOTE

Solution structure of an avirulence protein, AVR-Pia, from *Magnaporthe oryzae*

Toyoyuki Ose[1] · Azusa Oikawa[1] · Yukiko Nakamura[1] · Katsumi Maenaka[1] · Yuya Higuchi[2] · Yuki Satoh[2] · Shiho Fujiwara[2] · Makoto Demura[3] · Teruo Sone[2] · Masakatsu Kamiya[3]

Received: 26 June 2015 / Accepted: 18 August 2015 / Published online: 11 September 2015

Introduction

Plants have evolved to possess a two-layered innate immune system against diverse pathogens; this is a striking difference compared to higher animals that utilize mobile defender cells and a somatic adaptive immune system (Dangl et al. 2013; Dodds and Rathjen 2010; Jones and Dangl 2006). A plant's primary layer of defense is composed of pattern recognition receptors (PRRs). Once these proteins sense conserved pathogen (or microbial) associated molecular patterns (PAMPs or MAMPs), they initiate PAMP-triggered immunity (PTI). Pathogens, however, have evolved to suppress PTI by secreting effectors, i.e. inhibitory molecules (Chisholm et al. 2006). The sophisticated innate immune system of plants has coevolved with pathogens. The secondary layer of plant innate immunity (referred to as effector-triggered immunity, or ETI) employs plant resistance proteins (R-proteins) that recognize certain pathogen-derived effectors. This recognition promotes programmed cell death during the so-called hypersensitive response (HR) that occurs locally at infection sites. ETI is only activated when R-proteins successfully recognize a particular pathogenic species or when they are able to isolate specific pathogen effectors [the so-called avirulence (AVR) proteins]. Therefore, a detailed molecular analysis of the interaction between R and AVR proteins is essential for the development of foods, fibers, and biofuels, as well as for understanding plant immunity.

Rice blast caused by infection with the rice blast fungus, *Magnaporthe oryzae* (Couch), is the most devastating disease of rice worldwide (Dean et al. 2012). Mutations in its *AVR* genes allow *M. oryzae* to avoid the rice ETI system, since specific R-AVR interactions are perturbed (Sone et al. 2013). Bioinformatic analyses of the genomes of several rice strains have revealed approximately 500 genes encoding nucleotide binding and leucine-rich repeat (NB-LRR) proteins; this is the largest class of R proteins, and each family member contains NB and LRR domains (Monosi et al. 2004; Zhou et al. 2004). To date, around 100 rice *R* genes have been characterized, and 24 of these are involved in resistance to rice blast fungus (*Pib*, *Pita*, *Pi54*, *Pi-9*, *Pid2*, *Pi2*, *Piz-t*, *Pi-36*, *Pi-37*, *Pikm*, *Pi5*, *Pid3*, *Pi21*, *Pit*, *Pb1*, *Pish*, *Pi-k*, *Pik-p*, *Pia*, *NLS1*, *Pi25*, *Pi54rh*, *Pi54of*, and *Pid3-A4*) (Sharma et al. 2012). Among this 24-gene subset, 21 encode NBS-LRR family members, including rudimentary NBS-LRR such as *Pi54*, *Pi54rh*, and *Pi54of* (Das et al. 2012; Devanna et al. 2014). *Pi-d2* encodes a receptor-like kinase protein (Chen et al. 2006), and *Pi21* encodes a proline-rich protein (Fukuoka et al. 2009).

On the other hand, ten *AVR* genes have been cloned. These include *PWL1* (Kang et al. 1995), *PWL2* (Sweigard et al. 1995), *AVR-CO39* (Farman and Leong 1998), *AVR-Pita* (Orbach et al. 2000), *ACE1* (Fudal et al. 2005), *AVR-Pii* (Zhou et al. 2006), *AvrPiz-t* (Li et al. 2009), *AVR-Pia*

✉ Teruo Sone
sonet@chem.agr.hokudai.ac.jp

✉ Masakatsu Kamiya
mkamiya@sci.hokudai.ac.jp

[1] Faculty of Pharmaceutical Sciences, Hokkaido University, N12, W6, Kita-ku, Sapporo, Hokkaido 060-0812, Japan

[2] Graduate School of Agriculture, Hokkaido University, N9, W9, Kita-ku, Sapporo, Hokkaido 060-8589, Japan

[3] Faculty of Advanced Life Science, Hokkaido University, N10, W8, Kita-ku, Sapporo, Hokkaido 060-0810, Japan

(Miki et al. 2009), *AVR-Pik/km/kp* (Yoshida et al. 2009), and *AVR-Pi54* (Devanna et al. 2014). Direct interactions between *R* and *AVR* products, such as Pi-ta/AVR-Pita (Jia et al. 2000), Pik-1/AVR-Pik (Kanzaki et al. 2012), RGA5/AVR-CO39, and RGA5/AVR-Pia (Cesari et al. 2013) have already been described. Investigation of the NB-LRR paired protein RGA4/RGA5 system revealed that these proteins interact through their coiled-coil (CC) domains and form homo- and hetero-complexes (Cesari et al. 2014). Binding of AVR-CO39 or AVR-Pia to RGA5 causes segregation of RGA4–RGA5 hetero-complexes and promotes the formation of RGA4 homo-complexes, which ultimately leads to HR-induced death (Cesari et al. 2014). This is consistent with the role of RGA4 as an activator of both cell death and the HR (Cesari et al. 2014). To obtain further insight into R-AVR interactions at the molecular level, we constructed a recombinant AVR-Pia (rAVR-Pia) production system. We previously reported that rAVR-Pia expressed in *Escherichia coli* is trafficked to inclusion bodies, where it is denatured (Satoh et al. 2014). However, purification and refolding restores rAVR-Pia functionality, since the protein can trigger cell browning in leaves of the rice cultivar, Aichiasahi. Furthermore, an anti-AVR-Pia antibody raised against refolded rAVR-Pia can also detect native AVR-Pia secreted from *M. oryzae* Ina168 (Satoh et al. 2014). This confirms the quality of refolded AVR-Pia. Recently, analysis of the solution structure of AvrPiz-t revealed that it adopts a six-stranded β-sandwich fold with a pair of disulfide bonds (Zhang et al. 2013).

Here, we report the solution NMR structure of AVR-Pia. Surprisingly, the structure of AVR-Pia shows similarity to AvrPiz-t (Zhang et al. 2013) in topology regardless of the lack of amino acid sequence similarity between these two proteins. Concomitant with the presence of other structurally similar plant pathogens such as ToxB (Nyarko et al. 2014), our result indicates that there is a common mechanism in plants for recognizing effectors and leading to cell death.

Methods

Protein expression, purification, and NMR sample preparation

Uniformly $^{15}N/^{13}C$ enriched protein was refolded and purified under the same conditions as described previously for wild-type rAVR-Pia (Satoh et al. 2014). Briefly, the *E. coli* Rosetta (DE3) strain (Novagen) was transformed with pET-26b harboring rAVR-Pia cDNA and cultured in CHL medium-^{13}C, ^{15}N (Shoko Co., Ltd). For NMR spectroscopy, about 1 mM protein was prepared in 90 % H_2O/10 % D_2O containing 10 mM sodium phosphate buffer (pH 6.5) and 20 mM NaCl.

NMR data collection and assignments

All NMR spectra were recorded at 293–308 K either on a Bruker DMX 500 MHz equipped with a cryo-probe or a JEOL ECA 600 MHz spectrometer. Data were processed using NMRPipe 4.1 and NMRDraw 2.3 (Delaglio et al. 1995) and analyzed using Sparky 3.113 software (T. D. Goddard and D. G. Kneller, SPARKY 3, University of California, San Francisco, CA, USA). The assignment of the ^{1}H-, ^{13}C-, and ^{15}N resonances was carried out using the following set of spectra: [^{1}H–^{1}H] TOCSY, [^{1}H–^{1}H] NOESY, [^{1}H–^{15}N] heteronuclear single quantum coherence (HSQC), [^{1}H–^{13}C] HSQC, HNCO, HN(CO)CA, HNCA, CBCA(CO)NH, C(CO)NH, HBHA(CO)NH, and HC(C)H-TOCSY. All chemical shift values were referenced to 4,4-dimethyl-4-silapentane-1-sulfonic acid (DSS) and determined using these frequency ratios: ($^{15}N/^{1}H$) = 0.101329118, ($^{13}C/^{1}H$) = 0.251449519 (Wishart et al. 1995). The inter-proton distance restraints for the structural calculations were obtained from [^{1}H,^{1}H]-NOESY, ^{15}N-edited NOESY-HSQC, and ^{13}C-edited NOESY-HSQC spectra using a 150 ms mixing time.

NMR structure calculation

Distance restraints were derived from the inter-proton nuclear Overhauser effect (NOE). The restraints for the backbone phi and psi torsion angles were derived from the chemical shifts of the backbone atoms using the TALOS program (Shen et al. 2009). The structure was calculated using the CYANA 2.1 software package (Güntert 2004). A total of 784 distances and 104 angle restraints was used for the structure calculation. A total of 200 structures was calculated and a final ensemble of 20 structures was selected based on CYANA target function values. The quality of the final ensemble of structures was assessed with PROCHECK-NMR (Laskowski et al. 1996). The structures were visualized using PyMOL 1.7.4 (http://www.pymol.org/). Structure coordinates and NMR resonance assignments for AVR-Pia have been deposited in the BioMagResBank (BMRB) (entry 25636) and Protein Data Bank (PDB) (ID 2N37), respectively.

Relaxation measurements

The backbone ^{15}N relaxation parameters, including the longitudinal relaxation rate (R1), transverse relaxation rates (R2), and steady-state heteronuclear {^{1}H}–^{15}N NOE values of AVR-Pia were measured using standard pulse sequences on a Bruker Avance 600 MHz NMR spectrometer at 308 K. Recycle delays were set to 3 s for R1 and R2 experiments. The {^{1}H}–^{15}N NOE experiments were performed in the presence and absence of a 3-s proton

saturation period prior to the ^{15}N excitation pulse and using recycle delays of 2 and 5 s, respectively (Markley et al. 1971; Renner et al. 2002). The delays for the R1 were 2, 20, 60, 100, 300, 600, 1000, and 2000 ms. The delays for the R2 were 2, 20, 60, 90, 120, 150, 200, and 300 ms. The relaxation rate constants were obtained by fitting the peak intensities to a single exponential function using the non-linear least squares method. The rotational correlation time was estimated using the R2/R1 ratio by the r2r1_tm (http://www.palmer.hs.columbia.edu/software/quadric.html).

Results

Solution structure and dynamics of AVR-Pia

The ^{1}H–^{15}N HSQC spectrum of AVR-Pia acquired at pH 6.5 and 308 K was well dispersed, consistent with an ordered structure (Fig. 1). The assignment of the ^{1}H, ^{15}N, and ^{13}C resonances of AVR-Pia were essentially complete. Size exclusion chromatography indicated that it was a monomer under the conditions used in NMR experiments (data not shown). In addition, the rotational correlation time estimated from R2/R1 was 5.1 ± 0.4 ns. This value is comparable with the predicted value of a monomeric protein of similar size (Farrow et al. 1994). The solution structures of AVR-Pia were determined with NOE-derived distances and backbone dihedral angles (Table 1). Figure 2 shows the superposition of the final 20 energy-minimized AVR-Pia structures. The root-mean-square deviation (RMSD) from the mean structure in the structured region (residues 5–66) is 0.29 Å for the backbone atoms and 0.90 Å for all heavy atoms. The Ramachandran plot indicated that 76.3 % of residues are in the most favored regions, 23.7 % in the additionally allowed regions, and

Table 1 Structural statistics of AVR-Pia

Distance restraints	
Intra-residue (i = j)	228
Sequential (|i − j| = 1)	243
Medium (1 < |i − j| < 5)	75
Long range (|i − j| ≥ 5)	238
Total	784
Dihedral angle restraints	
Phi	52
Psi	52
Total	104
RMSD from mean (residues 5–66) (Å)	
Backbone	0.28 ± 0.08
Heavy atom	0.90 ± 0.10
Ramachandran plot (%)	
Residues in most favorable regions	76.3
Residues in additional allowed regions	23.7
Residues in generously allowed regions	0
Residues in disallowed regions	0

Structural statistics were computed by PROCHECK-NMR

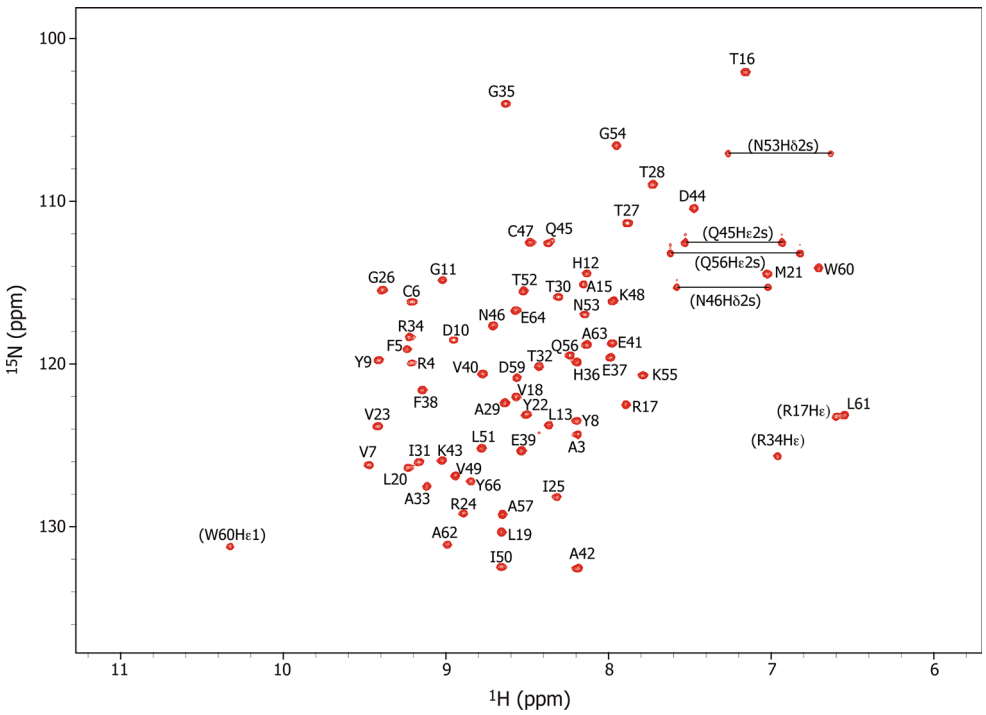

Fig. 1 The assigned ^{1}H–^{15}N HSQC spectrum of AVR-Pia acquired at 308 K. The assigned side chain resonances of Arg (Hε/Nε, aliased), Trp (Hε1/Nε1), Asn (Hδ2 s/Nδ2), and Gln (Hε2 s/Nε2) are indicated in *brackets*

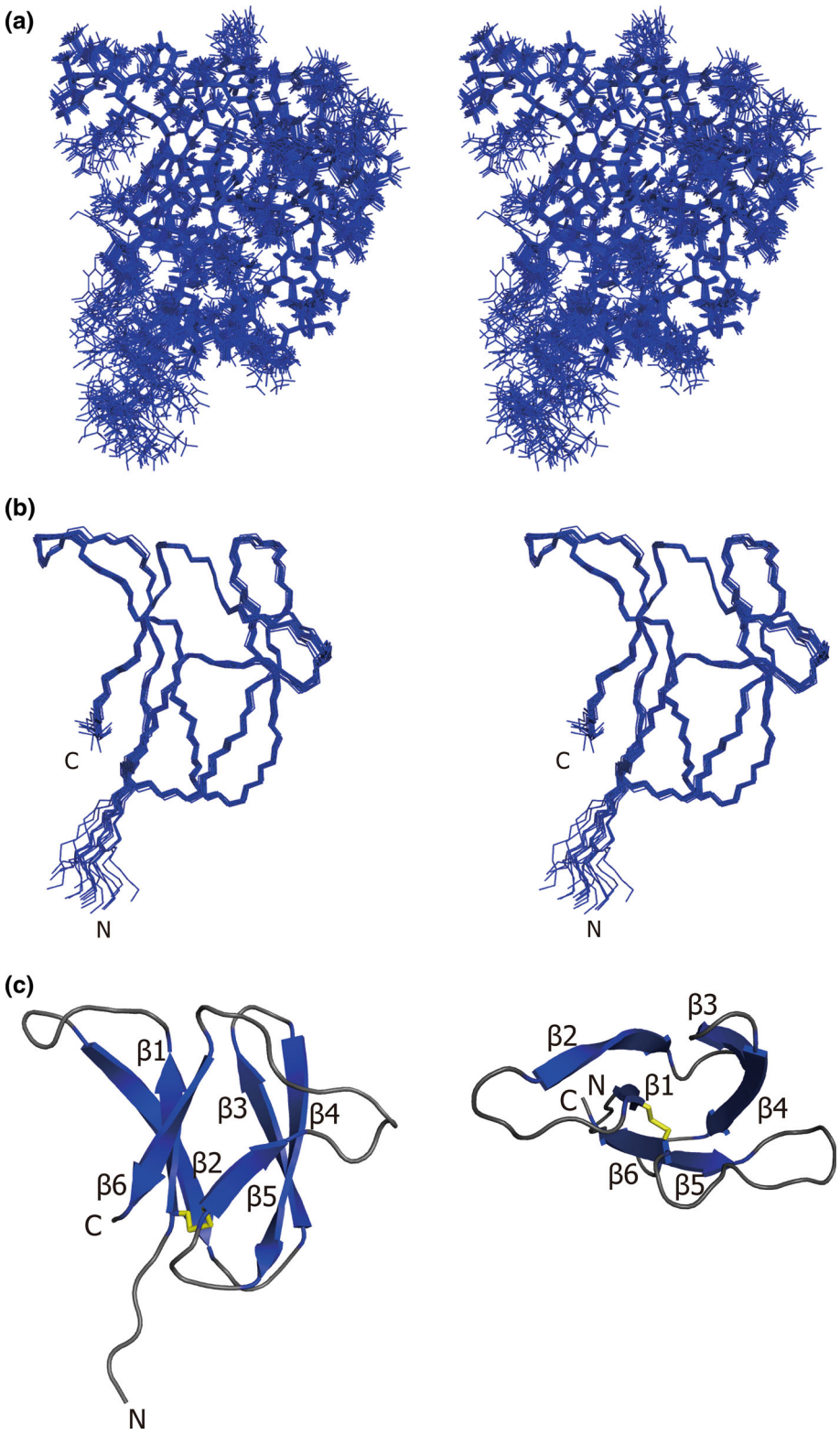

Fig. 2 Solution structure of AVR-Pia. **a** Stereoview of the ensemble of the 20 lowest energy structures of AVR-Pia. **b** Stereoview of the backbone atoms of AVR-Pia. **c** Ribbon diagram of the tertiary structure of AVR-Pia. The *yellow stick* indicates the disulfide bond between Cys 6 and Cys 47

none in the generously allowed regions and the disallowed regions.

AVR-Pia adopts a β-sandwich fold consisting of six anti-parallel β-strands corresponding to β1 (residues 6–10), β2 (residues 17–24), β3 (residues 28–33), β4 (residues 36–43), β5 (residues 47–50), and β6 (residues 61–65) stabilized by one disulfide bond between Cys 6 and Cys 47 (Fig. 2c). Strands β1, β2, and β6 form one-half of the

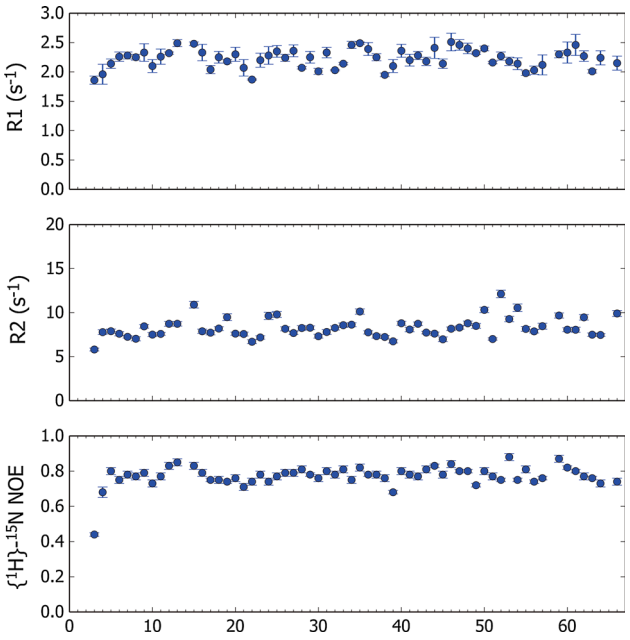

Fig. 3 Backbone relaxation parameters (R1, R2, and $\{^1H\}$–^{15}N heteronuclear NOE) of AVR-Pia. *Error bars* for R1 and R2 show fitting error. Errors for the NOE ratio were estimated from the root mean square variation of noise

sandwich, and β3, β4, and β5 form the other. A disulfide bond between Cys 6 in β1 and Cys 47 in β5 bridges each half. The overall region is rigid with an average R1 value of 2.22 s^{-1}, R2 of 8.27 s^{-1}, and an average $\{^1H\}$–^{15}N heteronuclear NOE of 0.78 (Fig. 3).

Discussion and conclusion

We used PDBeFold (Krissinel and Henrick 2004) to search for structures similar to AVR-Pia. This revealed that AVR-Pia has a similar fold to that of *Pyrenophora tritici-repentis* ToxB (PDBID: 2MM2) and *M. oryzae* AvrPiz-t (PDBID: 2lW6) as shown in Fig. 4. The RMSD values are 2.57 Å using 55 Cα atoms in ToxB and 2.76 Å using 51 Cα atoms in AvrPiz-t. There was no significant primary amino acid sequence similarity between these two proteins. However, they share a common six-stranded β-sandwich fold that is stabilized by a disulfide bond, in which β strands β1, β2, and β6 form an anti-parallel β-sheet, β3, β4, and β5 form the other anti-parallel β-sheet, and the two anti-parallel β-sheets sandwich a hydrophobic structural core (Zhang et al. 2013; Nyarko et al. 2014). These proteins share a common

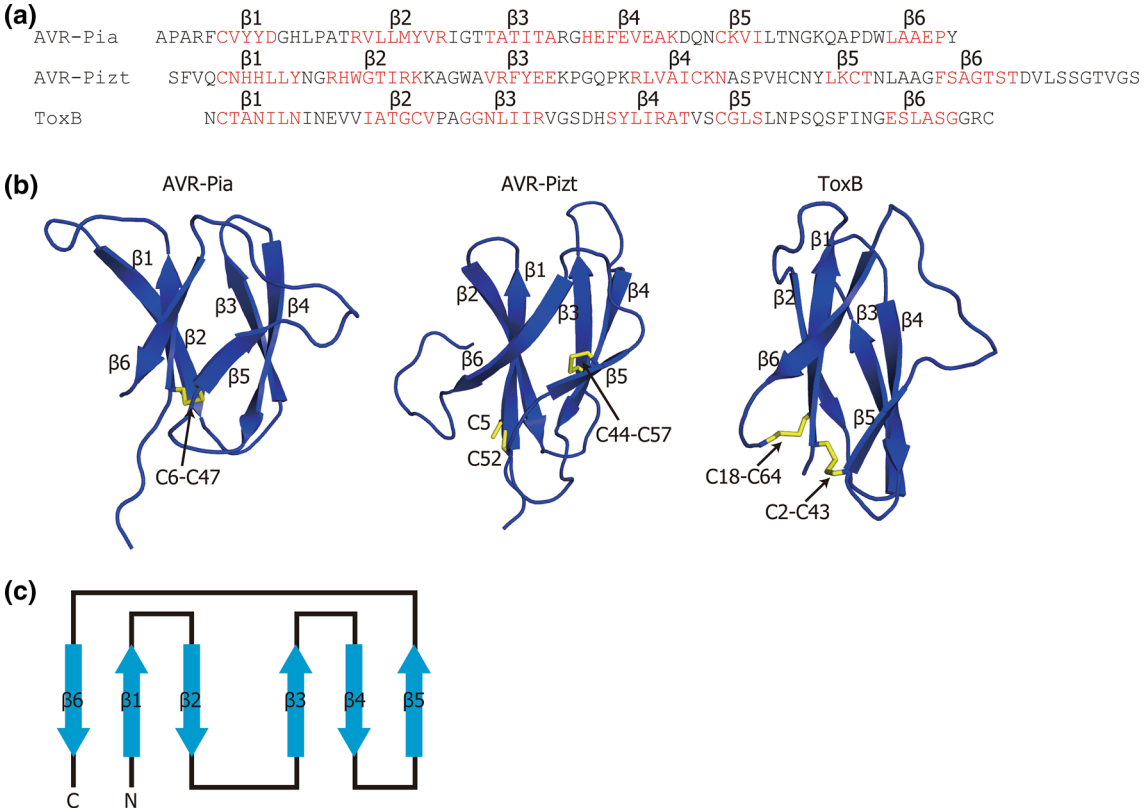

Fig. 4 Structural comparison of AVR-Pia with AvrPiz-t and ToxB. **a** Sequence alignment of AVR-Pia, AvrPiz-t, and ToxB. **b** Ribbon diagrams of AVR-Pia, AvrPiz-t (PDB ID 2LW6), and ToxB (PDB ID 2MM2). **c** Topology diagram of the structure

fold topology; however, the pattern of disulfide bonds is divergent. AVR-Pia has one disulfide bond between Cys 6 in β1 and Cys 47 in β5. In contrast, AvrPiz-t and ToxB have 4 cysteine residues forming two disulfide bonds: Cys 44 (β4)–Cys 57 (β5) and Cys 5 (β1)–Cys 52 (loop 4 between β4 and β5) in AvrPiz-t and Cys 2 (β1)–Cys 43 (β5) and Cys 18 (β2)–Cys 64 (C-terminus) in ToxB. All of these proteins have one cysteine in each of β1 and β5, and these cysteine residues form a disulfide bond in AVR-Pia and ToxB, but not in AvrPiz-t. This finding suggests that a disulfide bond between cysteines in β1 and β5 may not be required for the maintenance of structure and function of these proteins.

These proteins are important factors in the interaction between the producer fungi and their host plants. ToxB is described as a host-selective toxin, as it causes cell death in wheat genotypes with dominant toxin sensitivity genes and supports the virulence of necrotrophic *P. tritici-repentis*. *Magnaporthe oryzae* is a hemibiotrophic plant pathogen, which requires effectors for the suppression of the PTI system in the host and for successful infection. Effector activity for AVR-Pia has not been identified yet, but AVRPiz-t shows suppression of ROS generation upon chitin or flg22 treatment in transgenic rice, and its target protein has been identified (Park et al. 2012). AVR-Pia and AvrPiz-t are also known as avirulence effectors that trigger cell death in rice cultivars with their cognate dominant R genes and support the resistance of rice toward the pathogen. A mechanism of cell death induction by AVR-Pia/RGA5 direct interaction has been proposed (Cesari et al. 2014).

The structural similarity between ToxB and AvrPiz-t has already been reported (Nyarko et al. 2014). Together with the characterization of the AVR-Pia structure described here, these findings strongly suggest that these proteins utilize a common mechanism for interacting with host plant target proteins and causing cell death. Further structural studies of additional AVR protein family members will provide a greater understanding of their interaction with host proteins. Ultimately, this may inspire chemical biological strategies that can be applied to prevent crop loss due to infection.

Acknowledgments This work was supported by Grants-in-Aid for Scientific Research from the Ministry of Education, Culture, Sports, Science, and Technology of Japan (23380024), and the Program for Promotion of Basic and Applied Researches for Innovations in Bio-oriented Industry (BRAIN).

Compliance with ethical standards

Conflicts of interest The authors declare no conflict of interest.

References

Cesari S et al (2013) The rice resistance protein pair RGA4/RGA5 recognizes the *Magnaporthe oryzae* effectors AVR-Pia and AVR1-CO39 by direct binding. Plant Cell 25:1463–1481. doi:10.1105/tpc.112.107201

Cesari S et al (2014) The NB-LRR proteins RGA4 and RGA5 interact functionally and physically to confer disease resistance. EMBO J 33:1941–1959. doi:10.15252/embj.201487923

Chen X et al (2006) A B-lectin receptor kinase gene conferring rice blast resistance. Plant J 46:794–804. doi:10.1111/j.1365-313X.2006.02739.x

Chisholm ST, Coaker G, Day B, Staskawicz BJ (2006) Host-microbe interactions: shaping the evolution of the plant immune response. Cell 124:803–814. doi:10.1016/j.cell.2006.02.008

Dangl JL, Horvath DM, Staskawicz BJ (2013) Pivoting the plant immune system from dissection to deployment. Science 341:746–751. doi:10.1126/science.1236011

Das A, Soubam D, Singh PK, Thakur S, Singh NK, Sharma TR (2012) A novel blast resistance gene, Pi54rh cloned from wild species of rice, *Oryza rhizomatis* confers broad spectrum resistance to *Magnaporthe oryzae*. Funct Integr Genomics 12:215–228. doi:10.1007/s10142-012-0284-1

Dean R et al (2012) The Top 10 fungal pathogens in molecular plant pathology. Mol Plant Pathol 13:414–430. doi:10.1111/j.1364-3703.2011.00783.x

Delaglio F, Grzesiek S, Vuister GW, Zhu G, Pfeifer J, Bax A (1995) NMRPipe: a multidimensional spectral processing system based on UNIX pipes. J Biomol NMR 6:277–293

Devanna NB, Vijayan J, Sharma TR (2014) The blast resistance gene Pi54of cloned from *Oryza officinalis* interacts with Avr-Pi54 through its novel non-LRR domains. PLoS ONE 9:e104840. doi:10.1371/journal.pone.0104840

Dodds PN, Rathjen JP (2010) Plant immunity: towards an integrated view of plant-pathogen interactions. Nat Rev Genet 11:539–548. doi:10.1038/nrg2812

Farman ML, Leong SA (1998) Chromosome walking to the AVR1-CO39 avirulence gene of *Magnaporthe grisea*: discrepancy between the physical and genetic maps. Genetics 150:1049–1058

Farrow NA, Muhandiram R, Singer AU, Pascal SM, Kay CM, Gish G, Shoelson SE, Pawson T, Forman-Kay JD, Kay LE (1994) Backbone dynamics of a free and phosphopeptide-complexed Src homology 2 domain studied by ^{15}N NMR relaxation. Biochemistry 33:5984–6003

Fudal I, Bohnert HU, Tharreau D, Lebrun MH (2005) Transposition of MINE, a composite retrotransposon, in the avirulence gene ACE1 of the rice blast fungus *Magnaporthe grisea*. Fungal Genet Biol 42:761–772. doi:10.1016/j.fgb.2005.05.001

Fukuoka S et al (2009) Loss of function of a proline-containing protein confers durable disease resistance in rice. Science 325:998–1001. doi:10.1126/science.1175550

Güntert P (2004) Automated NMR Structure Calculation With CYANA. Protein NMR Techniques. Humana Press, New Jersey, pp 353–378

Jia Y, McAdams SA, Bryan GT, Hershey HP, Valent B (2000) Direct interaction of resistance gene and avirulence gene products confers rice blast resistance. EMBO J 19:4004–4014. doi:10.1093/emboj/19.15.4004

Jones JD, Dangl JL (2006) The plant immune system. Nature 444:323–329. doi:10.1038/nature05286

Kang S, Sweigard JA, Valent B (1995) The PWL host specificity gene family in the blast fungus *Magnaporthe grisea*. Mol Plant Microbe Interact 8:939–948

Kanzaki H et al (2012) Arms race co-evolution of *Magnaporthe oryzae* AVR-Pik and rice Pik genes driven by their physical interactions. Plant J 72:894–907. doi:10.1111/j.1365-313X.2012.05110.x

Krissinel E, Henrick K (2004) Secondary-structure matching (SSM), a new tool for fast protein structure alignment in three dimensions. Acta Crystallogr D Biol Crystallogr 60:2256–2268. doi:10.1107/S0907444904026460

Laskowski RA, Rullmannn JA, MacArthur MW, Kaptein R, Thornton JM (1996) AQUA and PROCHECK-NMR: programs for checking the quality of protein structures solved by NMR. J Biomol NMR 8:477–486

Li W et al (2009) The *Magnaporthe oryzae* avirulence gene AvrPiz-t encodes a predicted secreted protein that triggers the immunity in rice mediated by the blast resistance gene Piz-t. Mol Plant Microbe Interact 22:411–420. doi:10.1094/MPMI-22-4-0411

Markley JL, Horsley WJ, Klein MP (1971) Spin-Lattice relaxation measurements in slowly relaxing complex spectra. J Chem Phys 55:3604f (Chemical Measurements in Sl)

Miki S et al (2009) Molecular cloning and characterization of the AVR-Pia locus from a Japanese field isolate of *Magnaporthe oryzae*. Mol Plant Pathol 10:361–374. doi:10.1111/j.1364-3703.2009.00534.x

Monosi B, Wisser RJ, Pennill L, Hulbert SH (2004) Full-genome analysis of resistance gene homologues in rice. Theor Appl Genet 109:1434–1447. doi:10.1007/s00122-004-1758-x

Nyarko A et al (2014) Solution NMR structures of *Pyrenophora tritici*-repentis ToxB and its inactive homolog reveal potential determinants of toxin activity. J Biol Chem 289:25946–25956. doi:10.1074/jbc.M114.569103

Orbach MJ, Farrall L, Sweigard JA, Chumley FG, Valent B (2000) A telomeric avirulence gene determines efficacy for the rice blast resistance gene Pi-ta. Plant Cell 12:2019–2032

Park CH, Chen S, Shirsekar G, Zhou B, Khang CH, Songkumarn P, Afzal AJ, Ning Y, Wang R, Bellizzi M, Valent B, Wang GL (2012) The *Magnaporthe oryzae* effector AvrPiz-t targets the RING E3 ubiquitin ligase APIP6 to suppress pathogen-associated molecular pattern-triggered immunity in rice. Plant Cell 24:4748–4762. doi:10.1105/tpc.112.105429

Renner C, Schleicher M, Moroder L, Holak TA (2002) Practical aspects of the 2D ^{15}N–{^{1}H}-NOE experiment. J Biomol NMR 23:23–33. doi:10.1023/A:1015385910220

Satoh Y et al (2014) Heterologous production, purification, and immunodetection of *Magnaporthe oryzae* avirulence protein AVR-Pia. Biosci Biotechnol Biochem 78:680–686. doi:10.1080/09168451.2014.893186

Sharma TR, Rai AK, Gupta SK, Vijayan J, Devanna BN, Ray S (2012) Rice blast management through host-plant resistance: retrospect and prospects. Agric Res 1:37–52

Shen Y, Delaglio F, Cornilescu G, Bax A (2009) TALOS+: a hybrid method for predicting protein backbone torsion angles from NMR chemical shifts. J Biomol NMR 44:213–223. doi:10.1007/s10858-009-9333-z

Sone T et al (2013) Homologous recombination causes the spontaneous deletion of AVR-Pia in *Magnaporthe oryzae*. FEMS Microbiol Lett 339:102–109. doi:10.1111/1574-6968.12058

Sweigard JA, Carroll AM, Kang S, Farrall L, Chumley FG, Valent B (1995) Identification, cloning, and characterization of PWL2, a gene for host species specificity in the rice blast fungus. Plant Cell 7:1221–1233. doi:10.1105/tpc.7.8.1221

Wishart DS et al (1995) ^{1}H, ^{13}C and ^{15}N chemical shift referencing in biomolecular NMR. J Biomol NMR 6:135–140

Yoshida K et al (2009) Association genetics reveals three novel avirulence genes from the rice blast fungal pathogen *Magnaporthe oryzae*. Plant Cell 21:1573–1591. doi:10.1105/tpc.109.066324

Zhang ZM et al (2013) Solution structure of the *Magnaporthe oryzae* avirulence protein AvrPiz-t. J Biomol NMR 55:219–223. doi:10.1007/s10858-012-9695-5

Zhou T et al (2004) Genome-wide identification of NBS genes in japonica rice reveals significant expansion of divergent non-TIR NBS-LRR genes. Mol Genet Genomics 271:402–415. doi:10.1007/s00438-004-0990-z

Zhou B et al (2006) The eight amino-acid differences within three leucine-rich repeats between Pi2 and Piz-t resistance proteins determine the resistance specificity to *Magnaporthe grisea*. Mol Plant Microbe Interact 19:1216–1228. doi:10.1094/MPMI-19-1216